Development 139, 2340-2350 (2012) doi:10.1242/dev.070813

Von Hippel-Lindau protein in the RPE is essential for normal ocular growth and vascular development

Clemens A. K. Lange[1,2], Ulrich F. O. Luhmann[1], Freya M. Mowat[1], Anastasios Georgiadis[1], Emma L. West[1], Sabu Abrahams[3], Haroon Sayed[1], Michael B. Powner[3], Marcus Fruttiger[3], Alexander J. Smith[1], Jane C. Sowden[4], Patrick H. Maxwell[5], Robin R. Ali[1] and James W. B. Bainbridge[1,*]

SUMMARY

Molecular oxygen is essential for the development, growth and survival of multicellular organisms. Hypoxic microenvironments and oxygen gradients are generated physiologically during embryogenesis and organogenesis. In the eye, oxygen plays a crucial role in both physiological vascular development and common blinding diseases. The retinal pigment epithelium (RPE) is a monolayer of cells essential for normal ocular development and in the mature retina provides support for overlying photoreceptors and their vascular supply. Hypoxia at the level of the RPE is closely implicated in pathogenesis of age-related macular degeneration. Adaptive tissue responses to hypoxia are orchestrated by sophisticated oxygen sensing mechanisms. In particular, the von Hippel-Lindau tumour suppressor protein (pVhl) controls hypoxia-inducible transcription factor (HIF)-mediated adaptation. However, the role of Vhl/Hif1a in the RPE in the development of the eye and its vasculature is unknown. In this study we explored the function of Vhl and Hif1a in the developing RPE using a tissue-specific conditional-knockout approach. We found that deletion of *Vhl* in the RPE results in RPE apoptosis, aniridia and microphthalmia. Increased levels of Hif1a, Hif2a, Epo and Vegf are associated with a highly disorganised retinal vasculature, chorioretinal anastomoses and the persistence of embryonic vascular structures into adulthood. Additional inactivation of *Hif1a* in the RPE rescues the RPE morphology, aniridia, microphthalmia and anterior vasoproliferation, but does not rescue retinal vasoproliferation. These data demonstrate that Vhl-dependent regulation of Hif1a in the RPE is essential for normal RPE and iris development, ocular growth and vascular development in the anterior chamber, whereas Vhl-dependent regulation of other downstream pathways is crucial for normal development and maintenance of the retinal vasculature.

KEY WORDS: Von Hippel-Lindau factor, Hypoxia-inducible factor 1, Microphthalmia, Angiogenesis, Mouse

INTRODUCTION

Molecular oxygen is essential for the development, growth and survival of multicellular organisms. Hypoxic microenvironments and oxygen gradients are generated physiologically during embryogenesis and organogenesis. Tissue responses to local oxygen availability drive and coordinate the development of the blood, vasculature, the nervous system and other organs (Simon and Keith, 2008). In the eye, oxygen plays a crucial role in both physiological vascular development and common blinding neovascular diseases. Development of the retinal vasculature occurs in response to physiological hypoxia (Chan-Ling et al., 1995) generated by the increasing metabolic activity of differentiating neural cells (Stone et al., 1995). In the mature retina, phototransduction and intraretinal neuronal processing present a uniquely high metabolic demand for oxygen that is normally met by a highly efficient vascular supply. The photoreceptor cell layer in the outer retina is avascular and crucially dependent on the underlying choroidal circulation (Wangsa-Wirawan and Linsenmeier, 2003). Between the photoreceptor cell layer and the choroidal circulation lies the retinal pigmented epithelium (RPE), a monolayer of multifunctional cuboidal epithelial cells, and its basement (‘Bruch’s’) membrane. The RPE is developmentally derived from the outer layer of the bilayered optic cup, whereas the neuroretina develops from the inner layer. The periphery of the optic cup, including the presumptive RPE, contributes to the formation of the ciliary body and iris anteriorly. Normal development of the RPE is important for subsequent development of the choroidal vasculature (Gogat et al., 2004; Yi et al., 1998; Zhao and Overbeek, 2001) as well as closure of the optic fissure, retinal neurogenesis and neuronal cell projections (Bharti et al., 2006). Genetic ablation of the RPE or disruption of RPE specification genes during development in the mouse eye results in transdifferentiation to neuroretina, coloboma and microphthalmia (Bumsted and Barnstable, 2000; Martinez-Morales et al., 2001; Raymond and Jackson, 1995; Scholtz and Chan, 1987). In the adult, the mature RPE provides photoreceptor cells with metabolic support, recycles visual pigment, phagocytoses photoreceptor outer segment membranes, and maintains the blood-retina barrier and the health of the choroidal vasculature (Bharti et al., 2006; Marneros et al., 2005). Hypoxia at the level of the RPE has been proposed to play a crucial role in the regulation of pro-angiogenic cytokines, such as vascular endothelium growth factor (Vegf), and with the pathogenesis of age-related macular degeneration, which is the major cause of blindness in elderly people in industrialised countries (Arjamaa et al., 2009; Sheridan et al., 2009).

Oxygen homeostasis in mammals is maintained by highly sophisticated oxygen-sensing mechanisms that orchestrate adaptive tissue responses. The detection of hypoxia depends on the

[1]Department of Genetics, Institute of Ophthalmology, NIHR Biomedical Research Centre for Ophthalmology, University College London, London EC1V 9EL, UK. [2]University Eye Hospital Freiburg, Freiburg 79106, Germany. [3]Department of Cell Biology, Institute of Ophthalmology, NIHR Biomedical Research Centre for Ophthalmology, University College London, London EC1V 9EL, UK. [5]Division of Medicine, The Rayne Institute, University College London, London WC1E 6JF, UK. [4]Developmental Biology Unit, Institute of Child Health, University College London, London WC1N 1EH, UK.

*Author for correspondence (j.bainbridge@ucl.ac.uk)

Accepted 18 April 2012

interaction between the von Hippel-Lindau tumour suppressor protein (Pvhl) and hypoxia-inducible factors (HIFs). pVhl is a substrate recognition component of an E3-ubiquitin ligase protein that targets specific proteins and marks them for degradation. The most-studied target of pVhl is the family of HIFs, which play a major role in adaptive cellular responses to oxygen. HIFs are heterodimeric transcription factors, composed of one of three oxygen sensitive HIFa subunits (Hif1a, Hif2a and Hif3a), and the oxygen-insensitive and constitutively expressed HIFb subunit (Arnt). In normoxic conditions, Hifa subunits are hydroxylated by prolyl hydroxylases (PHDs) and subsequently ubiquitylated by the von Hippel-Lindau E3 ubiquitin ligase, which consequently leads to proteolytic destruction of Hif1a by the ubiquitin-proteasome pathway (Ivan et al., 2001; Maxwell et al., 1999). Under hypoxic conditions, this degradation does not occur and the accumulating Hif1a is translocated to the cell nucleus where it dimerises with the Hif1b subunit and enables the transcriptional activity of a wide range of genes involved in cellular metabolism, hypoxia tolerance and angiogenesis, including Vegf, erythropoietin (Epo) and platelet-derived growth factors (PDGFs) (Forsythe et al., 1996; Wang and Semenza, 1996; Zhang et al., 2003).

In this study, we have explored the function of Vhl and Hif1a in the developing RPE using a tissue-specific conditional knockout approach. Deletion of *Vhl* in the RPE results in microphthalmia, anterior segment developmental anomalies and vascular abnormalities. We demonstrate that Vhl expression in RPE is essential for the regulation of HIFs and Vegf, and is crucial for the development of both the eye and its circulatory system. Furthermore, by conditional inactivation of both *Vhl* and *Hif1a* in the RPE, we further delineate distinct roles of Vhl in the RPE and demonstrate Hif1a-dependent and Hif1a-independent functions that account for different components of the complex pathology.

MATERIALS AND METHODS

Animals

All animals were used with University College London ethics committee approval and under a UK Home Office project license and personal license. All procedures were performed in accordance with the Association for Research in Vision and Ophthalmology Statement for the Use of Animals in Ophthalmic and Vision Research. All mice in this study were maintained on a C57BL/6J background. Transgenic mice expressing cre recombinase under the control of the RPE cell-specific tyrosinase-related protein 1 promotor (*Tyrp1*, referred to as *C57BL/6$^{trp1\text{-}cre}$*) (Mori et al., 2002), were mated with *Vhl$^{floxed/floxed}$* (Haase et al., 2001), *Hif-1a$^{floxed/floxed}$* (Ryan et al., 2000) or double floxed *Vhl$^{floxed/floxed}$;Hif1a$^{floxed/floxed}$* mice. All experiments were controlled with age-matched littermates without the *trp1-cre* gene (referred to as control). The generation and genotyping of mice carrying the loxP-flanked conditional allele of *Vhl* and *Hif1a* was performed as previously described (Haase et al., 2001; Ryan et al., 2000).

Morphological examination of mouse eyes

In order to characterise the ocular development and eye growth of *Vhl$^{trp1\text{-}creKO}$*, *Vhl;Hif1a$^{trp1\text{-}creKO}$* and control mice, we assessed the eye diameter at different time points during development by measuring the distance from the optic nerve head to the centre of the cornea using an electronic digital caliper (range 5-10 animals per group per timepoint). To further characterise the ocular development macroscopically, we imaged the enucleated eyes of each genotype at different time points during development using a digital camera (Lumix 12×, DMC-TZ7, Panasonic).

Indocyanin green angiography

To analyse the ocular vascular phenotype in *Vhl$^{trp1\text{-}creKO}$*, *Vhl;Hif1a$^{trp1\text{-}creKO}$* and littermate control mice in vivo, we performed indocyanin green (ICG) angiography. Mice were anaesthetised by intraperitoneal injections of Dormitor (1 mg/ml, Pfizer Pharmaceuticals, Sandwich, UK) and ketamine (100 mg/ml, Fort Dodge Animal Health, Southampton, UK) mixed with sterile water in the ratio 5:3:42. Mice were injected with 0.2 ml ICG (5 mg/ml) in distilled water in the peritoneum and images were captured five minutes later using a HRA2 scanning laser ophthalmoscope (Heidelberg Engineering, Heidelberg, Germany) as previously described (Luhmann et al., 2009).

Electroretinography

To assess the retinal function of *Vhl$^{trp1\text{-}creKO}$*, *Vhl;Hif1a$^{trp1\text{-}creKO}$* and control mice, we recorded standard photopic and scotopic Ganzfeld electroretinography (ERG, range 5-8 per group) using the electrophysiological system Espion2000 (Espion E^2; Diagnosys, Cambridge, UK) as previously described (Carvalho et al., 2011).

Preparation of flatmount samples, cryo- and paraffin sections

Enucleated eyes were fixed in 4% PFA at room temperature for 10 minutes and dissected as previously described (Fruttiger et al., 1996; Gerhardt et al., 2003). Cryo- and paraffin sections of retinas were prepared as previously described (Mowat et al., 2010). For semi-thin and ultrastructural electromicroscopic (EM) analysis, animals were perfused with 3% glutaraldehyde and 1% PFA in 0.08 M sodium cacodylate-HCl (pH 7.4). Enucleated eyes were postfixed in the same fixative for at least 30 hours at 4°C followed by incubation in 1% aqueous osmium tetroxide for 2 hours. Tissue preparation and sectioning of semi-thin (0.7 μm) and ultrathin (70 nm) sections was performed as previously described (Luhmann et al., 2009).

Immunostaining and in situ hybridisation

Immunohistochemistry was performed as previously described (Mowat et al., 2010). The following primary antibodies were used: rabbit anti-collagen IV (2150-1470, AbD Serotec, Oxford, UK), rabbit anti-caspase 3 (ab 2302, Abcam, MA, USA), rabbit anti-cre (EMD Chemicals, Gibbstown, NJ, USA), mouse monoclonal anti-CtBP2 (BD Biosciences, Oxford, UK), rabbit anti-phospho-histone H3 (E173, Chemicon/Milipore, MA, USA), rabbit anti-GFAP (Dako UK, Cambridgeshire, UK), rabbit anti-Hif1a (Novus Biologicals Europe, Cambridge, UK), rabbit anti-Otx2 (Abcam, Cambridge, UK), rabbit anti-Pax6 (Covance, Princeton, NJ, USA), rabbit anti-recoverin (Chemicon/Milipore, MA, USA) and mouse anti-rhodopsin (Sigma Aldrich, Gillingham, UK). After extensive washing, sections were incubated with FITC- or TRITC-conjugated polyclonal goat anti-rabbit secondary or goat anti-mouse antibodies (Invitrogen, CA, USA) for 4 hours at room temperature and counterstained with 1 mg/ml DAPI (Invitrogen, CA, USA). Retinal flatmounts were stained with TRITC-conjugated isolectin B4 (Sigma-Aldrich, Gillingham, UK) or rabbit anti-Pecam (BD Pharmingen, CA, USA) in blocking medium overnight at 4°C. For evaluation of histology and ultrastructural analysis, paraffin sections were stained with Hematoxylin and Eosin, semi-thin sections with a 1% mixture of Toluidine Blue-borax in 50% ethanol, and ultrathin sections with saturated ethanolic uranyl acetate and lead citrate. In situ hybridisation on cryosections with a probe against full-length mouse *Vegf* mRNA (coding region and 3′ UTR) was carried out as previously described (West et al., 2005). Pigment in the RPE was subsequently bleached by incubating the sections first in $KMnO_4$ (0.25% in H_2O) for 10 minutes at room temperature and then in oxalic acid (1% in H_2O) for 20 min at room temperature.

Imaging and quantification

Fluorescence images were obtained using a confocal laser scanning microscope with a 20× or 40× water immersion plan apochromat lens (Zeiss LSM 710, Hertfordshire, UK). *Z*-stacks were 3D reconstructed and surface rendered using Imaris software (Bitplane, Zurich, Switzerland). For quantification of proliferating and apoptotic cells, the number of cell nuclei stained with caspase 3 or phospho-histone H3 were counted in the iris, retina and RPE in five central cryosections 60 μm apart. An average value per animal was calculated and used in subsequent analysis. Paraffin and semi-thin sections were imaged using a light microscope (Zeiss Axio Observer Z1, NY, USA), and the number of RPE cells on semi-thins was quantified as described above. For ultrastructural imaging, a transmission electron microscope (TEM model 1010; JEOL, Tokyo, Japan) was used

operating at 80 kV. All images were captured with a digital camera (QImaging micropublisher 5.0 digital camera, QImaging, BC, Canada) and exported as tiff files into Image J for quantification (developed by Wayne Rasband, National Institutes of Health, Bethesda, MD, USA; available at http://rsb.info.nih.gov/ij/index.html).

Real-time PCR

For real-time PCR, P0 eyes were homogenised and RNA was extracted using RNeasy Mini Kit (Qiagen, UK) and cDNA preparation was performed using the QuantiTect Reverse Transcription Kit (Qiagen, UK) according to manufacturer's instructions. Relative quantification by probe-based real-time PCR of the target genes (*Pax6*, *Mitf*, *Otx2*, *Epo*, *Flt1*, *Pdgfb* and *Vegf*) against endogenous β-actin expression levels was performed on 2 ng of cDNA using the following sets of primers:

murine *Pax6* forward, 5′-CAGTTCTCAGAGCCCCGTAT-3′;
murine *Pax6* reverse, 5′-CCACCAAGCTGATTCACTCC-3′;
murine *Mitf* forward, 5′-TGAGTGCCCAGGTATGAACA-3′;
murine *Mitf* reverse, 5′-GGATCCATCAAGCCCAAAA-3′;
murine *Otx2* forward, 5′-GGTATGGACTTGCTGCATCC-3′;
murine *Otx2* reverse, 5′-CGAGCTGTGCCCTAGTAAATG-3′;
murine *Epo* forward, 5′-TCTGCGACAGTCGAGTTCTG-3′;
murine *Epo* reverse, 5′-CTTCTGCACAACCCATCGT-3′;
murine *Flt1* forward, 5′-CCTCTGCATTTGGCATTAAGA-3′;
murine *Flt1* reverse, 5′-AGAGCTTTGTACTCACTGGCTGT-3′;
murine *Pdgfb* forward, 5′-CGGCCTGTGACTAGAAGTCC-3′;
murine *Pdgfb* reverse, 5′-GAGCTTGAGGCGTCTTGG-3′;
murine *Vegf* forward, 5′-GACTTGTGTTGGGAGGAGGA-3′;
murine *Vegf* reverse, 5′-TCTGGAAGTGAGCCAATGTG-3′;
murine β-actin forward, 5′-AAGGCCAACCGTGAAAAGAT-3′;
murine β-actin reverse, 5′-GTGGTACGACCAGAGGCATAC-3′.

Cyclic conditions were: 94°C for 30 seconds, 60°C for 1 minute, repeated for 40 cycles.

ELISA for Hif1a, Hif2a and Vegf

Eyes were collected at birth and immediately snap frozen in liquid nitrogen. After homogenisation in sterile PBS with protease inhibitors (Sigma-Aldrich, Gillingham, UK) using a pestle and a sonifier, the homogenate was spun at 5200 ***g*** for 10 minutes at 4°C and protein concentration of each sample was measured using a Lowry-based colorimetric protein assay performed in triplicate (DC protein assay kit, Bio-Rad, Hemel Hempstead, UK). Vegf, Hif1a and Hif2a protein levels were determined in the supernatant using commercially available ELISA kits (mouse HIF1a DuoSet, R&D Systems Europe, Abingdon, UK; HIF2a ELISA kit, Biorbyt, Riverside, UK; mouse VEGF DuoSet ELISA development kit, R&D Systems Europe, Abingdon, UK) according to manufacturer's instructions. The optical density of each sample was measured in triplicates at 450 nm with a reference at 650 nm using a microplate reader (Emax, Molecular Devices, Berkshire, UK) and compared with a standard curve of known concentration. To correct for total protein levels, we present Vegf, Hif1a and Hif2a protein levels per milligram of whole eye protein.

Statistical analysis

Comparison between the average variables of two groups was performed by a non-parametric Mann-Whitney U test. The average variables of more than two groups were compared by ANOVA with Tukey's test for multiple comparisons. *P* values less than 0.05 were considered statistically significant.

RESULTS

Conditional inactivation of *Vhl* in the RPE leads to Hif1a mediated aniridia and microphthalmia

To characterise the effect of *Vhl* inactivation in the RPE on eye development, we compared the eye size and the macroscopic phenotype of $Vhl^{trp1\text{-}creKO}$ mice and control littermates at time points during development. We observed abnormal ocular and iris development in $Vhl^{trp1\text{-}creKO}$ mice with 100% penetrance (Fig. 1A,B). The eye growth of $Vhl^{trp1\text{-}creKO}$ mice was similar to littermate controls during foetal development. Postnatally, however, $Vhl^{trp1\text{-}creKO}$ mice developed significant microphthalmia with a mean diameter of 2.1 ±0.13 mm (s.d.) compared with 3.0±0.21 mm (s.d.) in control mice at 1 month of age ($P<0.0001$, Fig. 1C). To evaluate the extent to which the observed phenotype in $Vhl^{trp1\text{-}creKO}$ mice is mediated by Hif1a, we generated mice with conditional inactivation of both *Vhl* and *Hif1a* in the RPE. This was achieved by crossing $Vhl;Hif1a^{flox/flox}$ mice with mice expressing cre recombinase under the control of the RPE-specific promoter *trp1*. $Vhl;Hif1a^{trp1\text{-}creKO}$ mice demonstrated normal iris and ocular development resulting in a normal postnatal ocular diameter of 2.8 ±0.22 mm (s.d.) at 1 month of age (Fig. 1A-C).

To assess the specificity of cre expression in the RPE, ocular sections of $C57BL/6^{trp1\text{-}cre}$ mice were stained for cre recombinase at E14.5. Strong expression of cre was evident in the RPE of $C57BL/6^{trp1\text{-}cre}$ mice and in a few neuroretinal cells of the distal optic cup, the primordium of the iris and ciliary body (Fig. 1D). To determine the effect of targeted deletion of *Vhl* in the developing RPE on ocular distribution of Hif1a and Vegf, Hif1a immunohistochemistry and Vegf in situ immunohistochemistry was performed on ocular sections of $Vhl^{trp1\text{-}creKO}$, $Vhl;Hif1a^{trp1\text{-}creKO}$ and littermate controls at E14.5. $Vhl^{trp1\text{-}creKO}$ mice demonstrated a strong activation of Hif1a in the RPE, which was absent in both $Vhl;Hif1a^{trp1\text{-}creKO}$ and control mice (Fig. 1E-J). In situ hybridisation demonstrated increased *Vegf* expression in the RPE of both $Vhl^{trp1\text{-}creKO}$ and $Vhl;Hif1a^{trp1\text{-}creKO}$ mice (Fig. 1K-M), indicating that RPE-specific inactivation of *Vhl* leads to a Hif1a-independent upregulation of Vegf in the RPE. Increased Vegf expression apparent in the neuroretina of these animals indicates secondary non-cell-autonomous effects that are independent of Hif1a.

To determine the concentration of the Vhl target proteins Hif1a, Hif2a and Vegf at the onset of microphthalmia, we measured protein concentration in the eyes of $Vhl^{trp1\text{-}creKO}$, $Vhl;Hif1a^{trp1\text{-}creKO}$ and control mice at P0 by ELISA. Hif1a, Hif2a and Vegf protein levels were significantly increased in $Vhl^{trp1\text{-}creKO}$ mice compared with littermate controls ($P=0.002$ for Hif1a, $P=0.01$ for Hif2a and $P=0.01$ for Vegf). By contrast, eyes of $Vhl;Hif1a^{trp1\text{-}creKO}$ mice had normal Hif1a levels but significantly increased Hif2a and Vegf protein levels compared with littermate controls ($P=0.01$ for Hif2a and Vegf, Fig. 1N). To determine further the effect of Hif stabilisation in the RPE on ocular levels of downstream target genes, we measured the expression of *Epo*, *Flt1*, *Pdgfb* and *Vegf* mRNA in the eyes of $Vhl^{trp1\text{-}creKO}$, $Vhl;Hif1a^{trp1\text{-}creKO}$ and control mice at P0 by real-time PCR. *Epo* mRNA levels were increased in both $Vhl^{trp1\text{-}creKO}$ and $Vhl;Hif1a^{trp1\text{-}creKO}$ mice compared with littermate controls ($P=0.03$). *Flt1* levels were increased in $Vhl^{trp1\text{-}creKO}$ mice compared with normal levels in $Vhl;Hif1a^{trp1\text{-}creKO}$ mice ($P=0.08$). *Pdgfb* and *Vegf* RNA levels were increased in both $Vhl^{trp1\text{-}creKO}$ and $Vhl;Hif1a^{trp1\text{-}creKO}$ mice although this did not reach statistical significance ($P=0.2$ for *Pdgfb*, $P=0.27$ for *Vegf*; Fig. 1O). Taken together, these data suggest that RPE-specific inactivation of *Vhl* leads to early activation of Hif1a, and a Hif1a-independent increase of Vegf in the RPE. Subsequently, a Hif1a-dependent increase in *Flt1* and Hif1a-independent increases in *Pdgfb*, *Vegf* and *Epo* levels suggest primary RPE-specific and secondary neuroretinal perturbation of angiogenic factors.

$Vhl^{trp1\text{-}creKO}$ mice exhibit severe abnormal ocular development and retinal degeneration

To elucidate further the developmental defect in $Vhl^{trp1\text{-}creKO}$ eyes, we examined H&E-stained paraffin sections of eyes at pre- and postnatal time points. Consistent with our findings on

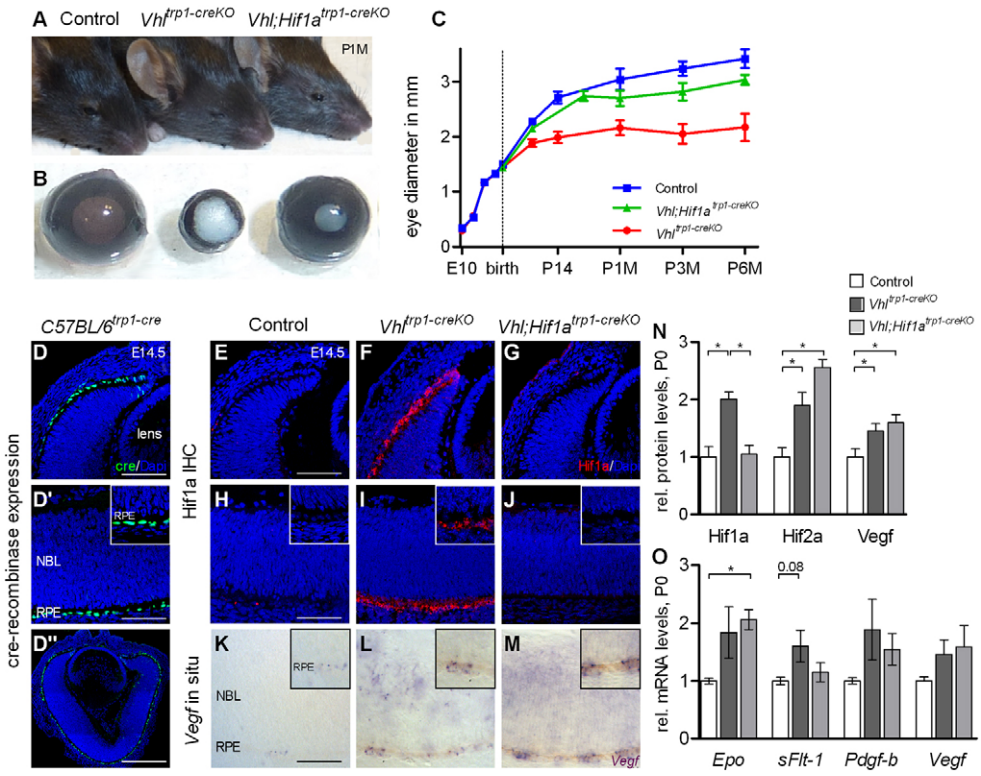

Fig. 1. *Vhl*$^{trp1\text{-}creKO}$ mice develop severe microphthalmia and aniridia that is rescued in *Vhl;Hif1a*$^{trp1\text{-}creKO}$ mice. (**A**,**B**) Representative images of *Vhl*$^{trp1\text{-}creKO}$, *Vhl;Hif1a*$^{trp1\text{-}creKO}$ mice, control mice and enucleated eyes at 1 month of age. (**C**) Timecourse of eye growth in *Vhl*$^{trp1\text{-}creKO}$ (red line), *Vhl;Hif1a*$^{trp1\text{-}creKO}$ (green line) and control mice (blue line). Data are mean±s.d. E, embryonic; P, postnatal; M, month. (**D-D″**) Representative cre immunohistochemistry in *C57BL/6*$^{trp1\text{-}cre}$ mice at E14.5 demonstrates specific cre expression in the RPE. Inset in D′ shows magnified view of RPE. (**E-J**) Representative Hif1a immunohistochemistry in *Vhl*$^{trp1\text{-}creKO}$, *Vhl;Hif1a*$^{trp1\text{-}creKO}$ and control mice at E14.5 shows RPE-specific activation of Hif1a in *Vhl*$^{trp1\text{-}creKO}$ mice that is absent in *Vhl;Hif1a*$^{trp1\text{-}creKO}$ and control mice. Insets show magnified view of RPE. (**K-M**) Representative *Vegf* in situ hybridisation demonstrating increased expression of *Vegf* in the RPE and neuroretina in *Vhl*$^{trp1\text{-}creKO}$ and *Vhl;Hif1a*$^{trp1\text{-}creKO}$ mice. Insets show magnified view of RPE. (**N**) Quantification of Hif1a, Hif2a and Vegf protein levels in *Vhl*$^{trp1\text{-}creKO}$, *Vhl;Hif1a*$^{trp1\text{-}creKO}$ and control mice at birth (four to six animals per group). (**O**) Quantification of *Epo*, *Flt1*, *Pdgfb* and *Vegf* mRNA levels in *Vhl*$^{trp1\text{-}creKO}$, *Vhl;Hif1a*$^{trp1\text{-}creKO}$ and control mice at birth (*n*=7 eyes per group). **P*<0.05. Data are mean±s.e.m. Scale bars: 75 μm in D,E-G; 50 μm in D′,H-M; 150 μm in D″.

macroscopic examination, we found rudimentary development of the iris and ciliary body and reduced RPE pigmentation in *Vhl*$^{trp1\text{-}creKO}$ eyes from E17 onwards (Fig. 2B,I). At E17, instead of the normal forward extension and thinning of the periphery of the optic cup demarcating the beginnings of the development of the ciliary body and iris, *Vhl*$^{trp1\text{-}creKO}$ mice show a lack of growth and forward extension of the pigmented layer and an abnormal backward folding extension of the neuroepithelium (Fig. 2I). Although the eye growth of *Vhl*$^{trp1\text{-}creKO}$ mice was significantly reduced during postnatal development, the lens developed normally and occupied the vitreous cavity and the anterior chamber from P7 onwards (Fig. 2N). By P7, the retina of *Vhl*$^{trp1\text{-}creKO}$ mice began to fold and form rosettes that increased over time in both number and size becoming most prominent at P31 (Fig. 2L,M). Adult *Vhl*$^{trp1\text{-}creKO}$ mice developed severe retinal degeneration with significant cell loss and retinal fibrosis (Fig. 2M,N). *Vhl;Hif1a*$^{trp1\text{-}creKO}$ mice, by contrast, developed a normal iris and ciliary body, and normal ocular growth with both anterior chamber and vitreous cavity and normal retinal lamination (Fig. 2O-U). Nonetheless, *Vhl;Hif1a*$^{trp1\text{-}creKO}$ developed mild irregularities in retinal layering in the periphery and remnant multilayered hyaloid vessels around the optic nerve head at P31 (Fig. 2T,U). These data indicate that Vhl-dependent Hif1a degradation in the RPE and pigmented iris precursor cells is essential for normal iris, RPE and ocular development that is otherwise associated with significant microphthalmia and retinal degeneration in the adult.

Embryonic inactivation of *Vhl* leads to Hif1a-mediated apoptosis of iris and RPE cells, which results in an abnormal morphology and reduced cell number

To determine the effect of *Vhl* inactivation on RPE morphology and survival, we characterised the RPE in further detail by semi-thin and ultrastructural analysis, and quantified apoptosis by caspase 3 immunohistochemistry at P0. In *Vhl*$^{trp1\text{-}creKO}$ mice, we measured a 60±4% (s.d.) reduction in the number of RPE cells (Fig. 3A,D,J; $P<0.0001$). Ultrastructural analysis revealed a dysmorphic RPE with dystrophic changes and a reduction in the content of melanin granules. The remaining granules appeared to be irregularly shaped, and melanin granules with the typical fusiform shape were scarce in number. Although the remaining RPE cells were sparse and the thickness of the RPE reduced, Bruch's membrane was preserved (Fig. 3B,E). Furthermore, we found a significant increase in the number of apoptotic cells in the RPE and in the pigmented iris in *Vhl*$^{trp1\text{-}creKO}$ mice ($P<0.0001$, Fig. 3C,F,K,M). The rate of apoptosis in the developing neural retina, however, was similar to that of littermate controls at birth ($P=0.22$,

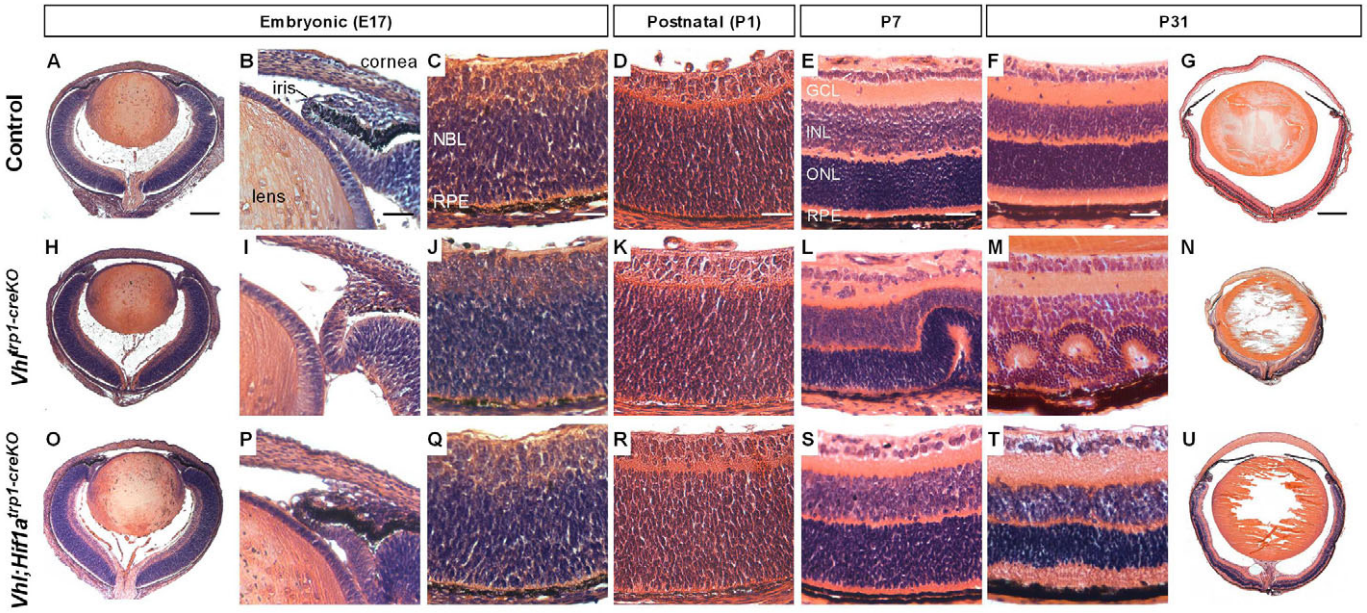

Fig. 2. *Vhl*$^{trp1\text{-}creKO}$ mice exhibit early defects in iris and RPE development that are associated with retinal degeneration and microphthalmia in the adult and are rescued in *Vhl;Hif1a*$^{trp1\text{-}creKO}$ mice. (**A-U**) Representative Haematoxylin and Eosin stained paraffin sections of control (A-G), *Vhl*$^{trp1\text{-}creKO}$ (H-N) *and Vhl;Hif1a*$^{trp1\text{-}creKO}$ mice (O-U) at different timepoints during development (five to eight animals per group). GCL, ganglion cell layer; NBL, neuroblast layer; INL, inner nuclear layer; ONL, outer nuclear layer; RPE, retinal pigmented epithelium. Scale bars: 250 μm in A,H,O; 25 μm in B,I,P; 20 μm in C,D,J,K,Q,R; 30 μm in E,F,L,M,S,T; 500 μm in G,N,U.

Fig. 3L). In *Vhl;Hif1a*$^{trp1\text{-}creKO}$ mice, by contrast, the RPE cell number and morphology, and the level of apoptosis in the RPE, iris and neuroretina, were all normal (Fig. 3G-M). These findings suggest that Hif1a-mediated cell death is responsible for reduction in RPE and pigmented iris cell number in *Vhl*$^{trp1\text{-}creKO}$ mice and indicates a crucial role for Vhl in regulating Hif1a levels for RPE, iris and eye development.

Embryonic inactivation of *Vhl* in the RPE reduces neuroretinal cell proliferation and affects the expression and localisation of Pax6 and Otx2 in the neuroretina

To determine the effect of RPE cell death in *Vhl*$^{trp1\text{-}creKO}$ mice on neuroretinal development, we assessed the rate of neuroretinal cell proliferation by phospho-histone H3 immunohistochemistry at birth. Conditional inactivation of *Vhl* in the RPE was associated with a significant reduction of mitotic cells at the ventricular surface of the developing retina compared with *Vhl;Hif1a*$^{trp1\text{-}creKO}$ mice and littermate controls (P=0.009, Fig. 4A-G). The level of proliferation in RPE and in the pigmented iris cells, however, was similar in *Vhl*$^{trp1\text{-}creKO}$, *Vhl;Hif1a*$^{trp1\text{-}creKO}$ and control mice (P=0.35, P=0.27, data not shown). These data demonstrate that RPE cell loss in *Vhl*$^{trp1\text{-}creKO}$ mice is associated with secondary effects on retinal development that may contribute to the development of microphthalmia.

As microphthalmia and aniridia have been associated with mutations in *Pax6* (Hill et al., 1991; Jordan et al., 1992), *Otx2* (Matsuo et al., 1995) and *Mitf* (Cheli et al., 2010), we investigated the cellular distribution of Pax6 and Otx2 by immunohistochemistry and the global expression levels of *Otx2*, *Pax6* and *Mitf* in the eyes of *Vhl*$^{trp1\text{-}creKO}$, *Vhl;Hif1a*$^{trp1\text{-}creKO}$ and control mice at birth by RT-PCR. Immunohistochemistry demonstrated a similar distribution of Pax6 in the central neuroretina of *Vhl*$^{trp1\text{-}creKO}$, *Vhl;Hif1a*$^{trp1\text{-}creKO}$ and control mice. Within the distal retina, i.e. the primordium of the iris, however, Pax6-expressing cells were reduced in number in *Vhl*$^{trp1\text{-}creKO}$ mice compared with *Vhl;Hif1a*$^{trp1\text{-}creKO}$ and control mice (Fig. 4I). *Pax6* RNA expression was also significantly decreased in *Vhl*$^{trp1\text{-}creKO}$ compared with control mice at birth (P=0.02, Fig. 4N). These data suggest that conditional inactivation of *Vhl* in the RPE and iris progenitor cells leads to reduced levels of Pax6-expressing cells in the distal part of the optic cup by birth that may contribute to the abnormal iris development.

Immunohistochemistry staining revealed similar Otx2 expression in the neuroretina of *Vhl*$^{trp1\text{-}creKO}$ and control mice, increased staining in the neuroretina of *Vhl;Hif1a*$^{trp1\text{-}creKO}$ mice, and normal staining in the RPE in both *Vhl*$^{trp1\text{-}creKO}$, *Vhl;Hif1a*$^{trp1\text{-}creKO}$ compared with control mice (Fig. 4O-T). Global *Otx2* RNA expression levels were also similar in *Vhl*$^{trp1\text{-}creKO}$ mice compared with control animals, suggesting that conditional inactivation of *Vhl* results in microphthalmia that may be independent of Otx2. Interestingly, global *Otx2* mRNA levels were increased twofold in *Vhl;Hif1a*$^{trp1\text{-}creKO}$ mice compared with *Vhl*$^{trp1\text{-}creKO}$ and control mice (P=0.0001, Fig. 4U), suggesting that other downstream molecules of Vhl influence neuroretinal Otx2 expression and localisation in a Hif1a-dependent manner. Furthermore RT-PCR analyses demonstrated similar global expression levels of *Mitf* in *Vhl*$^{trp1\text{-}creKO}$ and *Vhl;Hif1a*$^{trp1\text{-}creKO}$ eyes compared with littermate controls (P=0.5, data not shown). Although subtle and regional differences in Mitf expression cannot be excluded, these findings suggest that the development of microphthalmia in *Vhl*$^{trp1\text{-}creKO}$ mice may be independent of Mitf.

Taken together, these data highlight the crucial role of Vhl and Hif1a signalling in the RPE for normal ocular growth and iris development. The findings indicate that conditional inactivation of *Vhl* in the RPE leads to microphthalmia and aniridia, in a

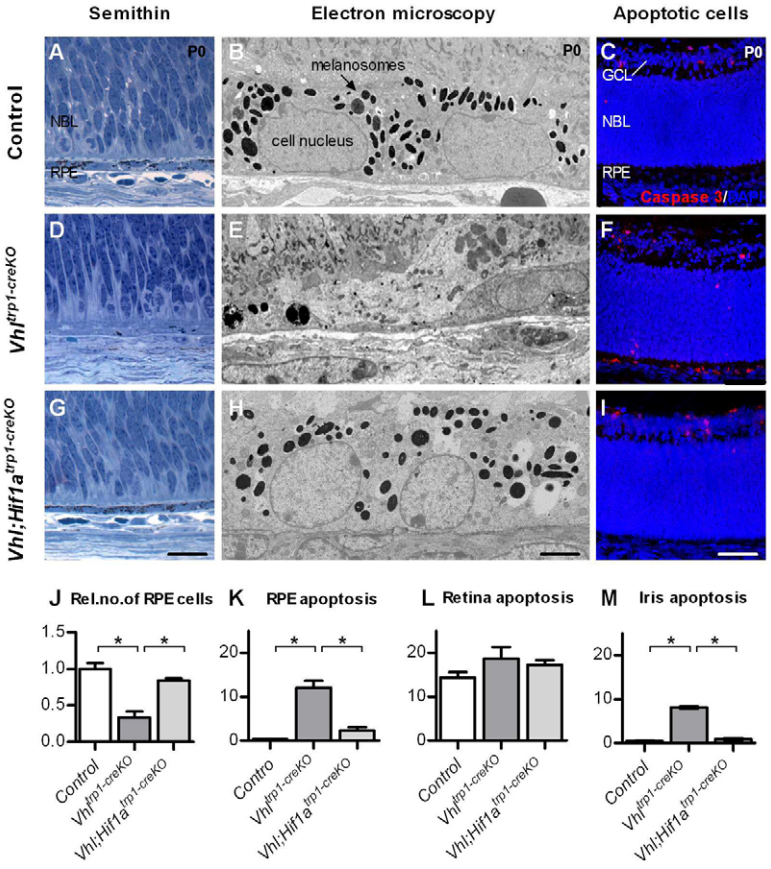

Fig. 3. *Vhl*$^{trp1\text{-}creKO}$ mice show reduced and dystrophic RPE cells with an increased rate of apoptosis compared with *Vhl;Hif1a*$^{trp1\text{-}creKO}$ and wild-type controls. (**A**,**B**,**D**,**E**,**G**,**H**) Semi-thin (A,D,G) and electron microscopy histology (B,E,H) show a dystrophic RPE and a reduced number of RPE cells in *Vhl*$^{trp1\text{-}creKO}$ compared with *Vhl;Hif1a*$^{trp1\text{-}creKO}$ and control mice at P0 (four to six animals per group). (**C**,**F**,**I**) Representative caspase 3 immunohistochemistry demonstrates increased apoptosis in the RPE and iris in *Vhl*$^{trp1\text{-}creKO}$ compared with *Vhl;Hif1a*$^{trp1\text{-}creKO}$ and control mice at birth. GCL, ganglion cell layer; NBL, neuroblast layer; RPE, retinal pigmented epithelium. Scale bars: 20 μm in A,D,G; 5 μm in B,E,H; 50 μm in C,F,I. (**J**) Quantification of the relative number of RPE cells in *Vhl*$^{trp1\text{-}creKO}$, *Vhl;Hif1a*$^{trp1\text{-}creKO}$ and control littermates at birth. (**K-M**) Quantification of apoptotic cells in the RPE (K), retina (L) and iris (M) in *Vhl*$^{trp1\text{-}creKO}$, *Vhl;Hif1a*$^{trp1\text{-}creKO}$ and control littermates at birth (four to six animals per group). *P<0.05. Data are mean±s.e.m.

mechanism that involves Hif1a-dependent increased RPE and iris apoptosis, reduced proliferation of retinal progenitor cells and reduced Pax6 expression in the distal optic cup.

Vhl$^{trp1\text{-}creKO}$ mice show persistence of the hyaloid vessels and the pupillary membrane

Having identified an early increase in the expression of angiogenic factors, we examined the vascular phenotype of *Vhl*$^{trp1\text{-}creKO}$ by in vivo ICG angiography and immunohistochemistry. In vivo ICG angiography demonstrated a perfused vascular network in the anterior chamber of *Vhl*$^{trp1\text{-}creKO}$ mice at P21 (Fig. 5E), consistent with a persistent pupillary membrane. However, collagen IV stained cryosections demonstrated vascular staining in the corneal stroma, indicating that this vasculature may be situated within the cornea (Fig. 5F). Additional inactivation of *Hif1a* in *Vhl;Hif1a*$^{trp1\text{-}creKO}$ mice rescued the vascular phenotype in the anterior part of the eye, demonstrating a normal vasculature of the iris and ciliary body and an avascular cornea (Fig. 5H,I). These data suggest that Vhl-mediated Hif1a regulation is essential for normal vascularisation of the anterior chamber.

Furthermore, *Vhl*$^{trp1\text{-}creKO}$ mice demonstrated persistent hyaloid vessels, disorganised retinal vessels with abrogated vascular lamination and retinal vessels growing into the outer retina (Fig. 6F-J). Whereas *Vhl;Hif1a*$^{trp1\text{-}creKO}$ mice developed normal vasculature in the anterior segment, they nonetheless exhibited a severely abnormal vascular phenotype in the retina. *Vhl;Hif1a*$^{trp1\text{-}creKO}$ mice developed persistent hyaloid vessels, a dense intraretinal vascular network with abrogated vascular lamination and retinal vessels in the outer retina similar to those observed in *Vhl*$^{trp1\text{-}creKO}$ mice (Fig. 6K-O; supplementary material Movies 1-3). To characterise the vascular phenotype in more detail, we examined the ocular vasculature on cryo-sections at time points during development. Compared with littermate controls, *Vhl*$^{trp1\text{-}creKO}$ mice developed normal retinal vasculature until P7, demonstrating a superficial vascular network and vessels diving into the outer plexiform layer in the central retina (Fig. 7B,F). In temporal association with the observed rosette formation, *Vhl*$^{trp1\text{-}creKO}$ mice also exhibit disorganised retinal vasculature and chorioretinal anastomoses from P14 onwards (Fig. 7G,H). *Vhl;Hif1a*$^{trp1\text{-}creKO}$ mice develop similarly disorganised retinal vasculature and chorioretinal anastomoses, as evident in *Vhl*$^{trp1\text{-}creKO}$ mice (Fig. 7K,L). Taken together, these data indicate that Vhl expression in the RPE contributes to normal layering of the retinal vasculature and maintenance of the blood-retina barrier that is independent of Hif1a in the RPE.

Adult *Vhl*$^{trp1\text{-}creKO}$ mice develop retinal degeneration which is partly dependent on Hif1a

To determine the long-term consequences of *Vhl* deletion in the RPE, we examined the retinal structure and function in adult *Vhl*$^{trp1\text{-}creKO}$ mice in detail by immunohistochemistry and electroretinography. Adult *Vhl*$^{trp1\text{-}creKO}$ mice (P8 weeks) develop a severe retinal degeneration with absent retinal lamination, reduced expression of rhodopsin and recoverin, and a reduced number of synapses (Fig. 8F-H). These morphological changes are associated with absent photopic and scotopic ERG function at all light intensities tested (Fig. 8I,J,P,Q). Additional inactivation of *Hif1a* in the RPE restores retinal lamination but does not abrogate GFAP activation, rhodopsin and recoverin expression, or restore normal synapse formation (Fig. 8K-M). This is associated with detectable scotopic a-waves at light intensities higher than 0.1 cd.s/m^2, indicating the presence of functioning photoreceptor cells, but

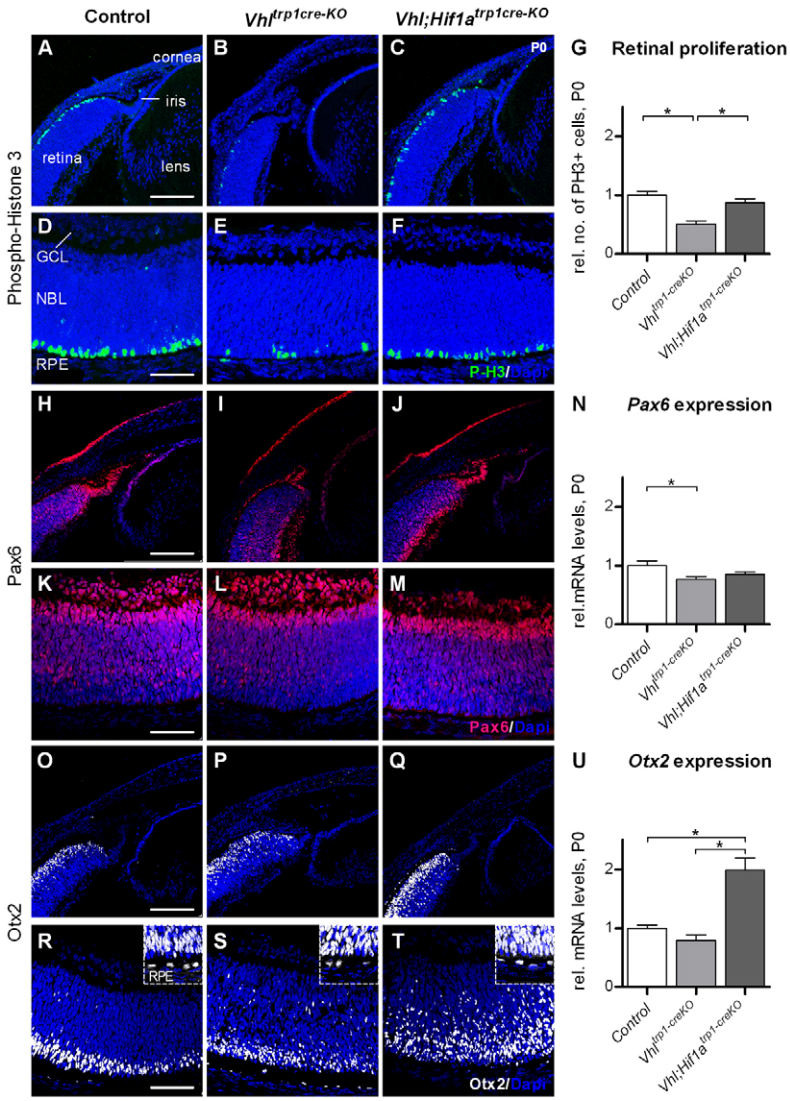

Fig. 4. Conditional inactivation of *Vhl* in the RPE decreases proliferation of retinal progenitor cells, and affects expression levels and localisation of Pax6 and Otx2 in the neuroretina. (**A-G**) Representative phospho-histone H3 immunohistochemistry (A-F) and quantification of proliferating cells (G) demonstrates a significant reduction of mitotic cells at the ventricular surface of the developing retina in *Vhl*$^{trp1\text{-}creKO}$ mice compared with *Vhl;Hif1a*$^{trp1\text{-}creKO}$ mice and littermate controls. (**H-M**) Pax6 immunohistochemistry demonstrates reduced Pax6 staining in the anterior retina in *Vhl*$^{trp1\text{-}creKO}$ mice compared with *Vhl;Hif1a*$^{trp1\text{-}creKO}$ and control mice. (**N**) Relative mRNA levels of *Pax6* are decreased *Vhl*$^{trp1\text{-}creKO}$ mice. (**O-T**) Otx2 immunohistochemistry shows a similar Otx2 distribution in *Vhl*$^{trp1\text{-}creKO}$ and control mice, and increased staining in *Vhl;Hif1a*$^{trp1\text{-}creKO}$ mice. (**U**) Relative mRNA levels of *Otx2* are increased in *Vhl;Hif1a*$^{trp1\text{-}creKO}$ mice. Scale bars: 150 μm in A-C,H-J,O-Q; 75 μm in D-F,K-M,R-T. GCL, ganglion cell layer; NBL, neuroblast layer; RPE, retinal pigmented epithelium. Data are mean ±s.e.m.; *P<0.05. Insets in R-T are magnified views of outer retina.

highly attenuated b-waves, consistent with reduced formation of synapses that is essential for bipolar cell activation (Fig. 8N-Q). These data suggest that, although secondary RPE cell death in the postnatal period may contribute to neuroretinal degeneration, Vhl expression in the RPE during development is crucial for the maturation of a normal functioning retina. Vhl-dependent Hif1a degradation in the RPE promotes normal retinal layering but does not appear to control maturation of the outer retina, which may depend on other Vhl-dependent factors such as Hif2a.

DISCUSSION

In the eye, oxygen plays a crucial role in both physiological vascular development and common blinding diseases. The RPE is essential for normal ocular development and is implicated in the pathogenesis of hypoxia-induced retinal disease. However, the role of the oxygen-sensing VHL/HIF-1a pathway in the RPE and its contribution to the development of the eye and its vasculature has not previously been examined. In this study, we investigated the function of Vhl and Hif1a in the developing RPE using a tissue-specific conditional knockout approach. We found that deletion of *Vhl* in the RPE results in a significant increase of Hif1a and Hif2a protein that is associated with a severe developmental phenotype, including the development of aniridia, microphthalmia and a strong pathological vascular phenotype in the anterior and posterior segments. Interestingly, aniridia, microphthalmia and the anterior vascular phenotype, but not the vascular phenotype in the retina, could be rescued by additional deletion of Hif1a in the RPE. These findings indicate that Vhl-dependent regulation of Hif1a in the RPE and pigmented iris cells is crucial for normal ocular and iris development, whereas other Vhl-dependent pathways in the RPE determine normal retinal vascularisation. The results also suggest that ocular hypoxia may be a previously unrecognised mechanism in the development of microphthalmia and that reduced systemic oxygenation, for example in placental insufficiency, could have important effects on ocular development through activation of HIFs in the RPE.

Our results demonstrate that conditional inactivation of *Vhl* in the RPE is associated with Hif1a-dependent increased apoptosis of RPE and pigmented iris cells. This finding is consistent with the results of recent studies showing that conditional inactivation of *Vhl* in the neuroretina is associated with increased apoptosis of photoreceptor cells (Kurihara et al., 2010; Lange et al., 2011). Hif1a regulates not only survival genes via its control of cellular proliferation and metabolism, vasomotor control and angiogenesis (Sharp and Bernaudin, 2004), but also the expression of pro-apoptotic factors. Hif1a can promote p53-mediated hypoxia-

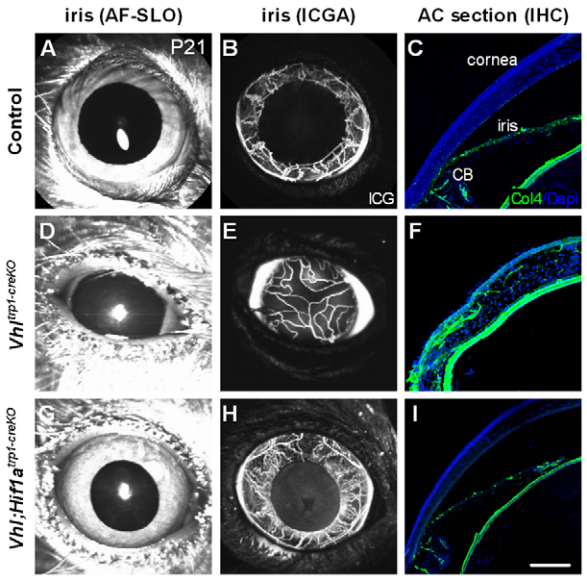

Fig. 5. *Vhl*$^{trp1\text{-}creKO}$ mice demonstrate a Hif1a-dependent persistence of the pupillary membrane. (**A-I**) Autofluorescence scanning laser ophthalmoscope (AF-SLO) imaging (A,D,G), indocyanin-green angiography (ICGA; B,E,H) and collagen IV-stained cryosections (C,F,I) of *Vhl*$^{trp1\text{-}creKO}$, *Vhl;Hif1a*$^{trp1\text{-}creKO}$ and control littermates at P21 show a persistent pupillary membrane in *Vhl*$^{trp1\text{-}creKO}$ mice that is absent in *Vhl;Hif1a*$^{trp1\text{-}creKO}$ and control mice. CB, ciliary body. Scale bar: 75 µm.

induced apoptosis in neurons of the CNS (Halterman et al., 1999), in part by upregulation of pro-apoptotic genes such as *Bnip3*, *Nix* (*Bnip3l* – Mouse Genome Informatics) and *Igfbp3*, and also by downregulation of anti-apoptotic genes such as *Bcl2* (An et al., 1998; Bacon and Harris, 2004; Carmeliet et al., 1998). These Hif1a-mediated pro-apoptotic mechanisms may be responsible for the RPE and iris cell loss in *Vhl*$^{trp1\text{-}creKO}$ mice, and contribute to the observed microphthalmia and aniridia. These results are consistent with the finding that toxic ablation of the RPE in vivo results in disorganisation of the retinal layer and an immediate arrest of eye growth (Raymond and Jackson, 1995). Furthermore, RPE cell loss in *Vhl*$^{trp1\text{-}creKO}$ mice may cause a secondary reduction in proliferating iris and retinal progenitor cells that could further contribute to the development of aniridia and microphthalmia.

Mutations in several transcription factors, including the microphthalmia-associated transcription factor (*Mitf*), the paired box gene 6 (*Pax6*) and the orthodenticle protein homolog 2 (*Otx2*) are associated with the development of aniridia and microphthalmia (Fuhrmann, 2010). *Mitf* plays a key role in melanocyte differentiation, proliferation and survival. Our findings demonstrate that conditional inactivation of *Vhl* in the RPE is associated with normal global expression levels of *Mitf*. Although we cannot exclude regional differences in Mitf expression in the eyes of *Vhl*$^{trp1\text{-}creKO}$ mice, these data suggest that conditional inactivation of *Vhl* in the RPE results in microphthalmia that may be independent of Mitf. *Pax6* is one of the key transcription factors involved in the complex process of eye development and plays multiple distinct roles in lens, iris and retinal development (Hever et al., 2006). Our results demonstrate that conditional inactivation of *Vhl* in the RPE is associated with a Hif1a-dependent reduction of Pax6 in the distal optic cup and pigmented iris primordium. Normal Pax6 expression in the distal optic cup is essential for iris development and reduced expression at this site results in iris hypoplasia (vis-Silberman et al., 2005). Our data suggest that a Hif1a-mediated loss of the RPE and the pigmented iris primordium can lead to reduced Pax6 expression in the distal optic cup and may therefore contribute to the absent iris development in *Vhl*$^{trp1\text{-}creKO}$ mice. Future studies will address the interaction of Vhl-Hif with the Pax6 pathway to elucidate further the developmental mechanisms responsible for aniridia. *Otx2* is a transcription factor involved in the regional specification of the eye, particularly in post-mitotic neuroblasts and in the RPE in early development (Martinez-Morales et al., 2001). Our results demonstrate that conditional inactivation of *Vhl* in the RPE does not affect Otx2 expression in the retina and RPE, suggesting that microphthalmia in *Vhl*$^{trp1\text{-}creKO}$ mice may be independent of Otx2. However, inactivation of both *Vhl* and *Hif1a* results in mislocalised and increased *Otx2* expression in the neuroretina, suggesting that other Vhl-dependent mechanisms may affect neuroretinal Otx2 expression and localisation in a Hif1a-dependent manner.

Our findings indicate that conditional inactivation of *Vhl* in the RPE results in severe retinal degeneration with undetectable photopic and scotopic ERG responses in adult mice. Additional inactivation of Hif1a in the RPE restores retinal lamination and detectable scotopic ERG a-wave responses that indicate the presence of functioning photoreceptor cells. The reduced number of synapses, which are essential for bipolar cell activation, in these animals may account for the persistent attenuation of ERG b-waves. These data suggest that Vhl expression in the RPE during development is crucial for the maturation of a normally functioning retina. Vhl-dependent Hif1a degradation in the RPE promotes normal retinal layering but does not appear to control maturation of the outer retina, which may depend on other Vhl-dependent factors such as Hif2a.

Whereas conditional inactivation of *Hif1a* in the RPE results in a normal ocular and vascular phenotype (Marneros et al., 2005), the conditional inactivation of *Vhl* in the RPE leads to striking anterior and posterior vascular changes. Adult *Vhl*$^{trp1\text{-}creKO}$ mice demonstrate persistence of the pupillary membrane and the hyaloid vasculature that usually regress early in development (Ito and Yoshioka, 1999). These embryonic vascular structures may persist in response to an early pro-angiogenic environment and high Vegf levels derived from RPE and pigmented iris cells, and subsequently in response to secondary changes in the neuroretina. Interestingly, the anterior vascular phenotype, but not the retinal vascular phenotype is rescued by additional conditional inactivation of *Hif1a*. This indicates an important primary role of Vhl-dependent Hif1a regulation for iris cell survival and the vascular development of the anterior chamber. The increased expression of Vegf and other angiogenic factors in the RPE and secondarily in the neuroretina in *Vhl*$^{trp1\text{-}creKO}$ mice may also be responsible for the dysmorphic and disorganised retinal vascular phenotype. Additional inactivation of *Hif1a* in the RPE did not abrogate Vegf overexpression in the RPE or neuroretina nor rescue the vascular phenotype. This indicates that other Vhl-regulated downstream molecules, such as Hif2a, may be responsible for Vegf expression in the RPE, the secondary increase of angiogenic factors in the neuroretina and the associated vascular phenotype. Retina-specific inactivation of *Vhl* leads to a similar but milder vascular phenotype, including the persistence of hyaloid vasculature and the pupillary membrane (Kurihara et al., 2010; Lange et al., 2011). In contrast to our results, Kurihara et al. reported that a combined inactivation of *Vhl* and *Hif1a* in the neuroretina rescues the vascular phenotype, suggesting that the observed phenotype was

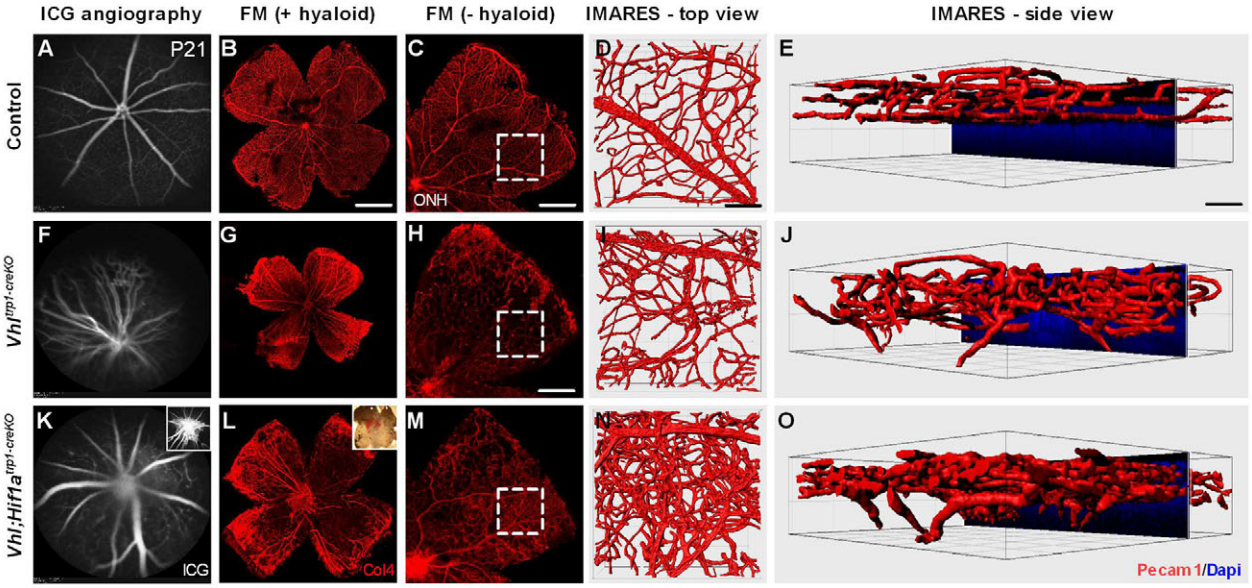

Fig. 6. *Vhl*$^{trp1\text{-}creKO}$ mice show a persistence of the hyaloid vasculature and a disorganised retinal vasculature that is independent of Hif1a. (**A**,**B**,**F**,**G**,**K**,**L**) Indocyanin-green angiography (A,F,K) and corresponding collagen 4-stained retinal flatmounts (B,G,L) show a persistent hyaloid vasculature in *Vhl*$^{trp1\text{-}creKO}$ and *Vhl;Hif1a*$^{trp1\text{-}creKO}$ mice that is absent in control littermates at P21. Inset in K shows angiography focussed on the persistent hyaloid vasculature. Inset in L shows a light microscopy image of a retinal flat mount with haemorrhage. (**C**,**H**,**M**) *Vhl*$^{trp1\text{-}creKO}$ and *Vhl;Hif1a*$^{trp1\text{-}creKO}$ mice demonstrate a disorganised retinal vasculature with areas of intra-retinal vascular proliferation compared with age-matched controls (hyaloid vessels were removed). Outlined regions indicate the areas selected for IMARES imaging. (**D**,**E**,**I**,**J**,**N**,**O**) IMARES reconstruction reveals a disorganised retinal vasculature with abrogated vascular layering and retinal vessels growing into the outer retina in *Vhl*$^{trp1\text{-}creKO}$ and *Vhl;Hif1a*$^{trp1\text{-}creKO}$ mice. Scale bars: 1 mm for B; 500 μm for C,M; 700 μm for H; 50 μm for D,E,I,J,N,O.

Hif1a mediated. This difference may be explained by the different localisation of *Vhl* inactivation (RPE versus neuroretina), indicating that the consequences of HIF1a stabilisation in the neuroretina differ from those of HIF1a in the RPE. Furthermore, our findings demonstrate that conditional inactivation of *Vhl* or *Vhl;Hif1* results in the secondary formation of chorioretinal anastomoses. These vascular malformations were evident from P10 onwards, although Hif1a and Vegf protein levels are already significantly unregulated at birth. Oshima et al. have shown that mice with overexpression of Vegf in RPE develop normal retinal and choroidal vasculature without spontaneous CNV formation. However, perturbation of the RPE and the Bruch's membrane by subretinal injection leads to the development of choroidal neovascularisation in transgenic mice overexpressing Vegf in the RPE (Oshima et al., 2004). Endogenous perturbation of the blood-retina barrier by Hif1a-mediated RPE cell death might promote the formation of chorioretinal anastomoses.

In conclusion, our results demonstrate for the first time the importance of the Vhl-Hif1a pathway in the RPE and pigmented iris for normal eye growth, iris development and vascular integrity.

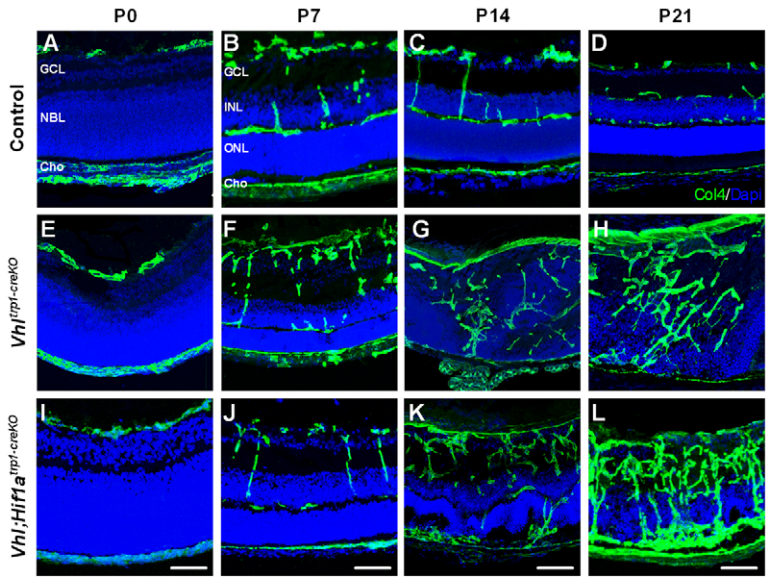

Fig. 7. Deletion of *Vhl* in the RPE results in disruption of the retinal vascular architecture and formation of chorioretinal anastomoses. (**A-L**) Representative collagen IV-stained cryosections of control (A-D), *Vhl*$^{trp1\text{-}creKO}$ mice (E-H) and *Vhl;Hif1a*$^{trp1\text{-}creKO}$ (I-L) and at different time points during development show a disorganised retinal vasculature and the formation of chorioretinal anastomoses in *Vhl;Hif1a*$^{trp1\text{-}creKO}$ and *Vhl*$^{trp1\text{-}creKO}$ mice (G,K). GCL, ganglion cell layer; NBL, neuroblast layer; Cho, choroid; INL, inner nuclear layer, ONL, outer nuclear layer. Scale bars: 25 μm.

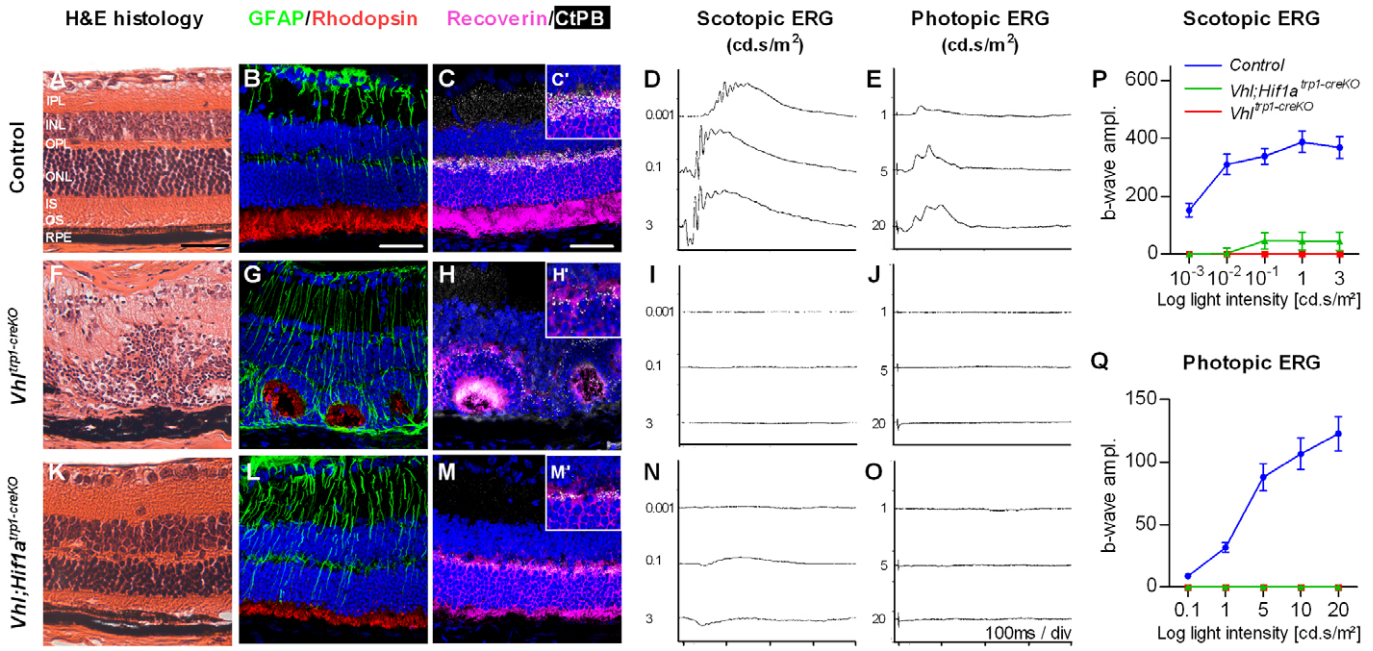

Fig. 8. *Vhl*$^{trp1\text{-}creKO}$ mice develop retinal degeneration in adults that is partly dependent on Hif1a. (**A-J**) Adult *Vhl*$^{trp1\text{-}creKO}$ mice demonstrate a complete retinal degeneration with absent retinal layering (F), increased GFAP activation and scarring (G), decreased rhodopsin and recoverin expression (G,H), and a reduction in synapses (H,H′), which is associated with absent photopic and scotopic ERG function (I,J), compared with littermate controls at 8 weeks of age (A-E). (**K-Q**) Additional inactivation of *Hif1a* in the RPE restores retinal layering (K) but results in increased GFAP activation (L), reduced rhodopsin and recoverin expression (L,M), and decreased synapsis formation (M,M′), which is associated with traces of a-waves at high light intensities in the scotopic ERG (N,P) and absent photopic ERG responses (O,Q). (P,Q) Mean b-wave amplitude (±s.e.m.) under photopic and scotopic condition at different light intensities. Scale bars: 50 μm in A-C. Scales: 0.2mV/div in D; 0.1mV/div in E.

Appropriate regulation of Hif1a by Vhl is essential for normal RPE and iris development, ocular growth and vascular development in the anterior chamber, whereas Vhl-dependent regulation of other downstream molecules is crucial for maintaining normal retinal vasculature.

Acknowledgements
We thank Dr Pierre Chambon for providing the *trp1-cre* mice and Yanai Duran for technical assistance.

Funding
This work was supported by The Wellcome Trust [074617/2/04/2]. R.R.A. and J.W.B.B. are supported by the National Institute for Health Research Biomedical Research Centre at Moorfields Eye Hospital and University College London Institute of Ophthalmology. J.C.S. is supported by Great Ormond Street Hospital Children's Charity. Deposited in PMC for release after 6 months.

Competing interests statement
The authors declare no competing financial interests.

Supplementary material
Supplementary material available online at
http://dev.biologists.org/lookup/suppl/doi:10.1242/dev.070813/-/DC1

References

An, W. G., Kanekal, M., Simon, M. C., Maltepe, E., Blagosklonny, M. V. and Neckers, L. M. (1998). Stabilization of wild-type p53 by hypoxia-inducible factor 1alpha. *Nature* **392**, 405-408.

Arjamaa, O., Nikinmaa, M., Salminen, A. and Kaarniranta, K. (2009). Regulatory role of HIF-1alpha in the pathogenesis of age-related macular degeneration (AMD). *Ageing Res. Rev.* **8**, 349-358.

Bacon, A. L. and Harris, A. L. (2004). Hypoxia-inducible factors and hypoxic cell death in tumour physiology. *Ann. Med.* **36**, 530-539.

Bharti, K., Nguyen, M. T., Skuntz, S., Bertuzzi, S. and Arnheiter, H. (2006). The other pigment cell: specification and development of the pigmented epithelium of the vertebrate eye. *Pigment Cell Res.* **19**, 380-394.

Bumsted, K. M. and Barnstable, C. J. (2000). Dorsal retinal pigment epithelium differentiates as neural retina in the microphthalmia (mi/mi) mouse. *Invest. Ophthalmol. Vis. Sci.* **41**, 903-908.

Carmeliet, P., Dor, Y., Herbert, J. M., Fukumura, D., Brusselmans, K., Dewerchin, M., Neeman, M., Bono, F., Abramovitch, R., Maxwell, P. et al. (1998). Role of HIF-1alpha in hypoxia-mediated apoptosis, cell proliferation and tumour angiogenesis. *Nature* **394**, 485-490.

Carvalho, L. S., Xu, J., Pearson, R. A., Smith, A. J., Bainbridge, J. W., Morris, L. M., Fliesler, S. J., Ding, X. Q. and Ali, R. R. (2011). Long-term and age-dependent restoration of visual function in a mouse model of CNGB3-associated achromatopsia following gene therapy. *Hum. Mol. Genet.* **20**, 3161-3175.

Chan-Ling, T., Gock, B. and Stone, J. (1995). The effect of oxygen on vasoformative cell division. Evidence that 'physiological hypoxia' is the stimulus for normal retinal vasculogenesis. *Invest. Ophthalmol. Vis. Sci.* **36**, 1201-1214.

Cheli, Y., Ohanna, M., Ballotti, R. and Bertolotto, C. (2010). Fifteen-year quest for microphthalmia-associated transcription factor target genes. *Pigment Cell Melanoma Res.* **23**, 27-40.

Forsythe, J. A., Jiang, B. H., Iyer, N. V., Agani, F., Leung, S. W., Koos, R. D. and Semenza, G. L. (1996). Activation of vascular endothelial growth factor gene transcription by hypoxia-inducible factor 1. *Mol. Cell. Biol.* **16**, 4604-4613.

Fruttiger, M., Calver, A. R., Kruger, W. H., Mudhar, H. S., Michalovich, D., Takakura, N., Nishikawa, S. and Richardson, W. D. (1996). PDGF mediates a neuron-astrocyte interaction in the developing retina. *Neuron* **17**, 1117-1131.

Fuhrmann, S. (2010). Eye morphogenesis and patterning of the optic vesicle. *Curr. Top. Dev. Biol.* **93**, 61-84.

Gerhardt, H., Golding, M., Fruttiger, M., Ruhrberg, C., Lundkvist, A., Abramsson, A., Jeltsch, M., Mitchell, C., Alitalo, K., Shima, D. et al. (2003). VEGF guides angiogenic sprouting utilizing endothelial tip cell filopodia. *J. Cell Biol.* **161**, 1163-1177.

Gogat, K., Le, G. L., Van Den, B. L., Marchant, D., Kobetz, A., Gadin, S., Gasser, B., Quere, I., Abitbol, M. and Menasche, M. (2004). VEGF and KDR gene expression during human embryonic and fetal eye development. *Invest. Ophthalmol. Vis. Sci.* **45**, 7-14.

Haase, V. H., Glickman, J. N., Socolovsky, M. and Jaenisch, R. (2001). Vascular tumors in livers with targeted inactivation of the von Hippel-Lindau tumor suppressor. *Proc. Natl. Acad. Sci. USA* **98**, 1583-1588.

Halterman, M. W., Miller, C. C. and Federoff, H. J. (1999). Hypoxia-inducible factor-1alpha mediates hypoxia-induced delayed neuronal death that involves p53. *J. Neurosci.* **19**, 6818-6824.
Hever, A. M., Williamson, K. A. and van, H. V. (2006). Developmental malformations of the eye: the role of PAX6, SOX2 and OTX2. *Clin. Genet.* **69**, 459-470.
Hill, R. E., Favor, J., Hogan, B. L., Ton, C. C., Saunders, G. F., Hanson, I. M., Prosser, J., Jordan, T., Hastie, N. D. and van, H. V. (1991). Mouse small eye results from mutations in a paired-like homeobox-containing gene. *Nature* **354**, 522-525.
Ito, M. and Yoshioka, M. (1999). Regression of the hyaloid vessels and pupillary membrane of the mouse. *Anat. Embryol. (Berl.)* **200**, 403-411.
Ivan, M., Kondo, K., Yang, H., Kim, W., Valiando, J., Ohh, M., Salic, A., Asara, J. M., Lane, W. S. and Kaelin, W. G., Jr (2001). HIFalpha targeted for VHL-mediated destruction by proline hydroxylation: implications for O2 sensing. *Science* **292**, 464-468.
Jordan, T., Hanson, I., Zaletayev, D., Hodgson, S., Prosser, J., Seawright, A., Hastie, N. and van, H. V. (1992). The human PAX6 gene is mutated in two patients with aniridia. *Nat. Genet.* **1**, 328-332.
Kurihara, T., Kubota, Y., Ozawa, Y., Takubo, K., Noda, K., Simon, M. C., Johnson, R. S., Suematsu, M., Tsubota, K., Ishida, S. et al. (2010). von Hippel-Lindau protein regulates transition from the fetal to the adult circulatory system in retina. *Development* **137**, 1563-1571.
Lange, C., Caprara, C., Tanimoto, N., Beck, S., Huber, G., Samardzija, M., Seeliger, M. and Grimm, C. (2011). Retina-specific activation of a sustained hypoxia-like response leads to severe retinal degeneration and loss of vision. *Neurobiol. Dis.* **41**, 119-130.
Luhmann, U. F., Robbie, S., Munro, P. M., Barker, S. E., Duran, Y., Luong, V., Fitzke, F. W., Bainbridge, J. W., Ali, R. R. and MacLaren, R. E. (2009). The drusenlike phenotype in aging Ccl2-knockout mice is caused by an accelerated accumulation of swollen autofluorescent subretinal macrophages. *Invest. Ophthalmol. Vis. Sci.* **50**, 5934-5943.
Marneros, A. G., Fan, J., Yokoyama, Y., Gerber, H. P., Ferrara, N., Crouch, R. K. and Olsen, B. R. (2005). Vascular endothelial growth factor expression in the retinal pigment epithelium is essential for choriocapillaris development and visual function. *Am. J. Pathol.* **167**, 1451-1459.
Martinez-Morales, J. R., Signore, M., Acampora, D., Simeone, A. and Bovolenta, P. (2001). Otx genes are required for tissue specification in the developing eye. *Development* **128**, 2019-2030.
Matsuo, I., Kuratani, S., Kimura, C., Takeda, N. and Aizawa, S. (1995). Mouse Otx2 functions in the formation and patterning of rostral head. *Genes Dev.* **9**, 2646-2658.
Maxwell, P. H., Wiesener, M. S., Chang, G. W., Clifford, S. C., Vaux, E. C., Cockman, M. E., Wykoff, C. C., Pugh, C. W., Maher, E. R. and Ratcliffe, P. J. (1999). The tumour suppressor protein VHL targets hypoxia-inducible factors for oxygen-dependent proteolysis. *Nature* **399**, 271-275.
Mori, M., Metzger, D., Garnier, J. M., Chambon, P. and Mark, M. (2002). Site-specific somatic mutagenesis in the retinal pigment epithelium. *Invest. Ophthalmol. Vis. Sci.* **43**, 1384-1388.
Mowat, F. M., Luhmann, U. F., Smith, A. J., Lange, C., Duran, Y., Harten, S., Shukla, D., Maxwell, P. H., Ali, R. R. and Bainbridge, J. W. (2010). HIF-1alpha and HIF-2alpha are differentially activated in distinct cell populations in retinal ischaemia. *PLoS ONE* **5**, e11103.
Oshima, Y., Oshima, S., Nambu, H., Kachi, S., Hackett, S. F., Melia, M., Kaleko, M., Connelly, S., Esumi, N., Zack, D. J. et al. (2004). Increased expression of VEGF in retinal pigmented epithelial cells is not sufficient to cause choroidal neovascularization. *J. Cell Physiol.* **201**, 393-400.
Raymond, S. M. and Jackson, I. J. (1995). The retinal pigmented epithelium is required for development and maintenance of the mouse neural retina. *Curr. Biol.* **5**, 1286-1295.
Ryan, H. E., Poloni, M., McNulty, W., Elson, D., Gassmann, M., Arbeit, J. M. and Johnson, R. S. (2000). Hypoxia-inducible factor-1alpha is a positive factor in solid tumor growth. *Cancer Res.* **60**, 4010-4015.
Scholtz, C. L. and Chan, K. K. (1987). Complicated colobomatous microphthalmia in the microphthalmic (mi/mi) mouse. *Development* **99**, 501-508.
Sharp, F. R. and Bernaudin, M. (2004). HIF1 and oxygen sensing in the brain. *Nat. Rev. Neurosci.* **5**, 437-448.
Sheridan, C. M., Pate, S., Hiscott, P., Wong, D., Pattwell, D. M. and Kent, D. (2009). Expression of hypoxia-inducible factor-1alpha and -2alpha in human choroidal neovascular membranes. *Graefes Arch. Clin. Exp. Ophthalmol.* **247**, 1361-1367.
Simon, M. C. and Keith, B. (2008). The role of oxygen availability in embryonic development and stem cell function. *Nat. Rev. Mol. Cell Biol.* **9**, 285-296.
Stone, J., Itin, A., Alon, T., Pe'er, J., Gnessin, H., Chan-Ling, T. and Keshet, E. (1995). Development of retinal vasculature is mediated by hypoxia-induced vascular endothelial growth factor (VEGF) expression by neuroglia. *J. Neurosci.* **15**, 4738-4747.
vis-Silberman, N., Kalich, T., Oron-Karni, V., Marquardt, T., Kroeber, M., Tamm, E. R. and shery-Padan, R. (2005). Genetic dissection of Pax6 dosage requirements in the developing mouse eye. *Hum. Mol. Genet.* **14**, 2265-2276.
Wang, G. L. and Semenza, G. L. (1996). Molecular basis of hypoxia-induced erythropoietin expression. *Curr. Opin. Hematol.* **3**, 156-162.
Wangsa-Wirawan, N. D. and Linsenmeier, R. A. (2003). Retinal oxygen: fundamental and clinical aspects. *Arch. Ophthalmol.* **121**, 547-557.
West, H., Richardson, W. D. and Fruttiger, M. (2005). Stabilization of the retinal vascular network by reciprocal feedback between blood vessels and astrocytes. *Development* **132**, 1855-1862.
Yi, X., Mai, L. C., Uyama, M. and Yew, D. T. (1998). Time-course expression of vascular endothelial growth factor as related to the development of the retinochoroidal vasculature in rats. *Exp. Brain Res.* **118**, 155-160.
Zhang, S. X., Gozal, D., Sachleben, L. R., Jr, Rane, M., Klein, J. B. and Gozal, E. (2003). Hypoxia induces an autocrine-paracrine survival pathway via platelet-derived growth factor (PDGF)-B/PDGF-beta receptor/phosphatidylinositol 3-kinase/Akt signaling in RN46A neuronal cells. *FASEB J.* **17**, 1709-1711.
Zhao, S. and Overbeek, P. A. (2001). Regulation of choroid development by the retinal pigment epithelium. *Mol. Vis.* **7**, 277-282.